Kinetic analysis of histone acetylation turnover and Trichostatin A induced hyper- and hypoacetylation in alfalfa

Jakob H. Waterborg and Tamás Kapros

Abstract: Dynamic histone acetylation is a characteristic of chromatin transcription. The first estimates for the rate of acetylation turnover of plants are reported, measured in alfalfa cells by pulse, pulse-chase, and steady-state acetylation labeling. Acetylation turnover half-lives of about 0.5 h were observed by all methods used for histones H3, H4, and H2B. This is consistent with the rate at which changes in gene expression occur in plants. Treatment with histone deacetylase inhibitor Trichostatin A (TSA) induced hyperacetylation at a similar rate. Replacement histone variant H3.2, preferentially localized in highly acetylated chromatin, displayed faster acetyl turnover. Histone H2A with a low level of acetylation was not subject to rapid turnover or hyperacetylation. Patterns of acetate labeling revealed fundamental differences between histone H3 versus histones H4 and H2B. In H3, acetylation of all molecules, limited by lysine methylation, had similar rates, independent of the level of lysine acetylation. Acetylation of histones H4 and H2B was seen in only a fraction of all molecules and involved multiacetylation. Acetylation turnover rates increased from mono- to penta- and hexaacetylated forms, respectively. TSA was an effective inhibitor of alfalfa histone deacetylases in vivo and caused a doubling in steady-state acetylation levels by 4–6 h after addition. However, hyperacetylation was transient due to loss of TSA inhibition. TSA-induced overexpression of cellular deacetylase activity produced hypoacetylation by 18 h treatment with enhanced acetate turnover labeling of alfalfa histones. Thus, application of TSA to change gene expression in vivo in plants may have unexpected consequences.

Résumé : L'acétylation dynamique des histones est une caractéristique de la transcription de la chromatine. Cet article présente les premières estimations du taux de renouvellement des groupes acétyle chez les plantes, obtenues en mesurant l'acétylation grâce à un marquage bref, suivi ou non d'une chasse, et à un marquage à l'équilibre de cellules de luzerne. La demi-vie de renouvellement des groupes acétyle des histones H3, H4 et H2B est environ 0,50 h selon toutes les méthodes. Cela concorde avec la vitesse de modification de l'expression des gènes chez les plantes. Une incubation en présence de Trichostatine A (TSA), un inhibiteur des histones désacétylases, induit une hyperacétylation à une vitesse similaire. Le taux de renouvellement des groupes acétyle de l'histone H3.2 de remplacement, qui se trouve préférentiellement dans la chromatine hyperacétylée, est plus rapide. L'histone H2A peu acétylée a un taux de renouvellement des groupes acétyle lent et elle n'est pas sujette à l'hyperacétylation. Le marquage avec l'acétate montre qu'il y a des différences fondamentales entre l'histone H3, d'une part, et les histones H4 et H2B, d'autre part. L'acétylation de toutes les molécules d'histone H3, limitée par la méthylation des résidus lysine, se fait à la même vitesse, indépendamment du niveau d'acétylation des résidus lysine. Par contre, seulement une fraction de toutes les molécules des histones H4 et H2B sont acétylées et cela fait intervenir de multiples acétylations. Les taux de renouvellement des groupes acétyle augmentent en allant des formes mono-acétylées aux formes penta- et hexa-acétylées. La TSA est un bon inhibiteur des histones désacétylases de la luzerne in vivo et le taux d'acétylation à l'équilibre double 4 à 6 h après traitement avec la TSA. Cependant, l'hyperacétylation est transitoire car l'inhibition par la TSA disparaît progressivement. La TSA induit la surexpression des désacétylases cellulaires, ce qui engendre une hypoacétylation, 18 h aprés traitement avec la TSA, et une augmentation du taux de renouvellement des groupes acétyle des histones de la luzerne. Donc, l'application de TSA à des plantes afin de modifier l'expression de leurs gènes in vivo pourrait avoir des conséquences imprévues.

[Traduit par la Rédaction]

Introduction

Histone acetylation is recognized as one of the important factors that allow gene transcription in a chromatin environment. Chromatin, the packaging of DNA by histones, presents a formidable obstacle to gene transcription (Orphanides and Reinberg 2000). Initially, Allfrey and co-workers recognized that lysine acetylation of histones, detected through ra-

Received 31 December 2001. Revised 26 February 2002. Accepted 7 March 2002. Published on the NRC Research Press Web site at http://bcb.nrc.ca on 17 April 2002.

J.H. Waterborg[1] and T. Kapros. Division of Cell Biology and Biophysics, School of Biological Sciences, University of Missouri, Kansas City, MO 64110, U.S.A.

[1]Corresponding author (e-mail: WaterborgJ@umkc.edu).

 DOI: 10.1139/O02-021 © 2002 NRC Canada

dioactive acetate labeling in vivo and quantitated as bands with reduced gel electrophoretic mobility in acetic acid-urea gels, correlated with gene transcription in animal cells (Allfrey 1977). They speculated that the elimination of the lysine charge would release tight binding to DNA, allowing RNA polymerases to transcribe genes. They observed that acetylation was a rapid, posttranslational modification. Recently, the role of acetylation in chromatin transcription has been widened by the recognition that histone acetyl-lysines provide specific attachment sites for transcription factors containing bromo domains, providing an essential framework for the assembly of transcription initiation complexes (Dhalluin et al. 1999; Jacobson et al. 2000; Matangkasombut et al. 2000). They are part of the site-specific signals that interact with other functional modifications like phosphorylation and ubiquitination (Mizzen and Allis 2000; Strahl and Allis 2000). They organize directly or indirectly through coactivator transcription factors the various histone acetyltransferase (HAT) enzymes that increase the level of histone acetylation locally, apparently relaxing the repressive character of the nucleosomes, allowing nucleosome remodeling and transcription (Nightingale et al. 1998; Brown et al. 2000; Fax et al. 2000; Hecht et al. 2000; Kurooka and Honjo 2000). Conversely, transcriptional corepressors have been shown to bring in tethered histone deacetylase (HDAC) enzymes to repressed or silenced genes (Wade et al. 1998; Ayer 1999; Bird and Wolffe 1999; Doetzlhofer et al. 1999; Gilbert and Sharp 1999; Ahringer 2000). The progression of a high acetylation state across transcribed chromatin may be established through HATs associated with transcribing RNA polymerases (Wittschieben et al. 1999; Orphanides and Reinberg 2000). In addition, HATs may produce the domain-wide increases in chromatin acetylation observed for the chicken β-globin locus (Hebbes and Allen 2000). It is clear that histone acetylation must be very dynamic and that changes in histone acetylation at promoters mirror rapid changes in gene expression (Kadosh and Struhl 1997; Pazin and Kadonaga 1997; Kuo et al. 1998; Richon et al. 2000).

In animal cells, fast rates of histone acetylation and deacetylation have been measured with half-lives as short as 3 min (Jackson et al. 1975; Chestier and Yaniv 1979; Zhang and Nelson 1988*a*, 1998*b*; Hendzel and Davie 1991). Recently, we have demonstrated through dynamic steady-state acetylation labeling that the vast majority of acetyl-lysines in the chromatin of the green alga *Chlamydomonas reinhardtii* is rapidly turning over with half-lives of 2–4 minutes (Waterborg 1998). Histone acetylation in the yeast *Saccharomyces cerevisiae* had been thought to be rather static with acetylation and deacetylation rates of several hours (Nelson 1982). However, with the development of a new method to retain histone acetylation quantitatively (Waterborg 2000), it has been possible to measure acetylation turnover rates for yeast histones with half-lives of 15 min for histone H4, 10 min for H3, and 5 min for histones H2B and H2A (Waterborg 2001). These latter studies have revealed that acetylation of histone H3 may be different from acetylation of histones H4 and H2B. The rates of acetylation turnover at every level of acetylation in histone H3 are the same and almost all H3 acetylation is dynamic. In contrast, the rate and extent of acetylation turnover of multiacetylated H4 and H2B histones are much higher than measured for low or monoacetylated forms. In this paper, we show through data collected in alfalfa (*Medicago varia*) A2 cell culture that this difference between histones H4 and H2B versus histone H3 is also observed in plants and thus may represent a fundamental difference in histone functions within the nucleosome.

In recent years, histone acetylation has been studied in a variety in plants (Arfmann and Haase 1981; Idei et al. 1996; Ransom and Walton 1997; Belyaev et al. 1998; Buzek et al. 1998; Vyskot et al. 1999). We had chosen alfalfa as a model system, partially based on a very robust tissue cell culture of A2 cells (Waterborg et al. 1989; Kapros et al. 1995). The distinct difference in histone acetylation levels of two histone H3 variants (Waterborg et al. 1987, 1989; Waterborg 1992*a*) has lead to the identification of a constitutively expressed histone variant, named H3.2, which exists in all monocot and dicot plants (Waterborg 1991, 1992*a*). Its function is to maintain transcribed genes in a chromatin context (Waterborg 1993*a*). The formation of replacement nucleosomes on transcribed sequences, denuded of nucleosomes, results in enhanced histone acetylation, characteristic of transcriptionally active chromatin. This paper presents a direct comparison of the dynamic characteristics of histone acetylation between the abundant, moderately acetylated, replication-dependent histone variant H3.1, assembled into newly replicated chromatin (Waterborg 1993*a*; Kapros et al. 1995), and the highly acetylated replacement histone variant H3.2, which is assembled into nucleosomes within transcribing chromatin and frequently lost during subsequent transcription (Waterborg 1993*a*).

To date, the turnover rate of histone acetylation has not been determined for any plant, including alfalfa, even though acetate labeling of alfalfa histones has been used extensively (Waterborg et al. 1987, 1990; Waterborg 1992*a*, 1993*a*). Acetate labeling has been a tool to study the functional expression of the replication-dependent histone variant H3.1 (Waterborg 1993*a*; Kapros et al. 1995), to demonstrate the characteristically high acetylation of the replacement H3.2 in transcribed chromatin (Waterborg 1993*a*), and to demonstrate that all five lysines in the unmethylated amino terminus of histone H4 are subject to acetylation, a feature common to plants and algae (Waterborg 1992*b*, 1998).

In animal cells the HDAC inhibitor butyric acid has been used to induce hyperacetylation and to determine the rate of deacetylation upon butyrate withdrawal (Schroter et al. 1981; Covault et al. 1982). This method cannot be used in alfalfa because butyrate is rapidly metabolized into acetyl-CoA (Waterborg et al. 1990). Increased histone acetylation was observed in response to butyrate in tobacco (Arfmann and Haase 1981) but not in artichoke (Pedersen and Minocha 1988). With the recognition that fungal metabolites such as Trichostatin A (TSA) and HC toxin are inhibitors of many HDACs (Brosch et al. 1995), although not all (Sanchez-del-Pino et al. 1994; Carmen et al. 1996, 1999; Lechner et al. 1996; Lusser et al. 2001), these compounds have been used in plants. They have been shown to affect histone acetylation in maize (Ransom and Walton 1997) and beans (Belyaev et al. 1997, 1998). In this paper, we present the responses of alfalfa to TSA, including a sequential pattern of histone hyperacetylation and hypoacetylation that results from metabolic inactivation of the inhibitor.

© 2002 NRC Canada

Materials and methods

Histone preparation and analysis

Throughout this study, alfalfa A2 suspension cultures were used as described (Waterborg 1993*a*). Translation inhibitor cycloheximide was used at a final concentration of 10 μg/mL MS growth medium, added 10 min before addition of acetate from fresh, nonsterile stock (2 mg/mL in ethanol). For labeling at reduced specific radioactivity, 0.1 M NH_4Ac was added 30 min prior to the addition of tritiated acetate to the final concentration specified for each experiment. High specific activity [^{3}H]NaAc (1.5×10^{14} Bq/mol, NEN Life Science Products, Boston, Mass.) was used as specified in each experiment. TSA (Wako Bioproducts, Richmond, Va.) was dissolved in dimethyl sulfoxide at 0.5 mg/mL (1.67 mM), stored at –20°C, and used at the concentrations specified in each experiment. Histones were extracted from whole cells, collected by centrifugation into chaotropic guanidine hydrochloride (pH 6.8), purified by Bio-Rex 70 (Bio-Rad, Richmond, Calif.) chromatography, dialyzed into 2.5% acetic acid with 0.1 mL 2-mercaptoethanol/L, and lyophilized as described (Waterborg 1990, 1993*a*). Histones were fractionated into pools of crude histone H2B, histone H4 with H2A, and histone H3 by reversed-phase high-pressure liquid chromatography (HPLC) on Zorbax Protein-Plus as described (Waterborg 1993*a*, 2000). The specific radioactivity of fractions was determined by liquid scintillation counting and optical density measurements at 214 nm (Waterborg 2000). Following lyophilization, histones were analyzed on acetic acid–urea–Triton (AUT) gels (Waterborg 1990, 1998) by densitometry of Coomassie staining and fluorography, as described elsewhere (Waterborg et al. 1995; Waterborg 1998). Multiple preflashed fluorography exposures were made from each gel to obtain specific radioactivity measurements within the linear range of fluorography and X-ray film dynamics. SigmaPlot for Windows, version 5.00 (SPSS Inc., Chicago, Ill.), was used for linear and nonlinear regression analyses. Data presented met all statistical tests for convergence and fit.

Results

Acetate labeling of alfalfa histones

Acetylated histones can be isolated from whole cells of alfalfa A2 cultures by a chaotropic extraction method in guanidine hydrochloride that prevents proteolysis of histone polypeptides and loss of modifications like lysine acetylation (Waterborg et al. 1987, 1989). Fractionated by reversed-phase HPLC, all four core histones are obtained in a fairly to highly pure state (Waterborg 1992*b*, 1993*a*) as a fraction with histone H2B, as a fraction of histone H4 with histone H2A, and as two fractions of the separated histone H3.1 and H3.2 variants (Waterborg 1990). The latter fractions were combined if analysis required determination of the ratio between the two variant forms. Gel electrophoresis in acetic AUT polyacrylamide gels was routinely employed to separate histones from each other, such as histone H2A from histone H4, and to allow quantitation of the distribution of acetylated forms. Figure 1 (lane A) shows a typical example of the Coomassie staining pattern of AUT gels.

Fig. 1. Acetylation pattern of alfalfa histones by Coomassie staining and acetate fluorography of AUT gels. Alfalfa A2 cells (50-mL aliquot) were made 10 μg/mL in cycloheximide. After 10 min, 0.5 mCi of tritiated acetate was added to 4 μM. After 5 min, cells were collected by centrifugation. Histones were extracted and fractionated by HPLC into H3, H4–H2A, and H2B preparations that were run on long AUT gels. Lane A shows the Coomassie-stained composite of H3, H4, H2B, and H2A gel regions, with the corresponding fluorograph in lane B. The histone names and variant forms are shown for each gel segment. Lines mark each level of charge modification visible in either lane with numbers at the lowest and highest visible levels of acetylation. Ammonium acetate was added to 0.4 mM to parallel aliquots. Cells were collected by centrifugation and resuspended for continued culture in MS medium supplemented with 0.4 mM ammonium acetate. Samples were collected after various times and histone fluorographs are shown for histones after a chase period of 10 min (lane C), 25 min (lane D), 60 min (lane E), and 120 min (lane F). Fluorography exposures shown were developed after 3 days for H3 histones and after 17 days for all other histones.

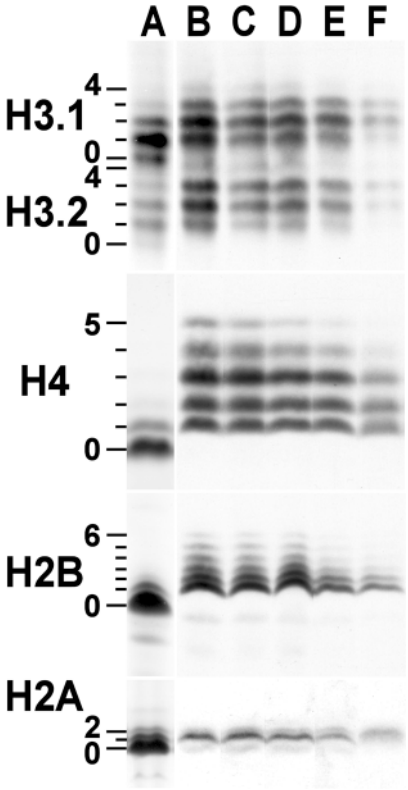

Triacetylated forms are typically the highest modified forms visible in stained patterns of histones H3.1, H3.2, H4, and H2B, even though the distribution pattern of modified bands differs. Histone H3.1 and H3.2 variants typically contain, on average, 0.5–0.7 and 1.0–1.5 acetyl-lysines, respectively, while histone H4 contains 0.4 and histone H2B carries 0.25 acetyl-lysines. The charge-modified forms of histone H2A are partially caused by phosphorylation (Waterborg et al. 1989).

Labeling of alfalfa cells with tritiated acetate reveals up to five acetylated lysines, i.e., all five lysines in the amino terminus of histone H4 (Waterborg 1992*b*), and suggests that

© 2002 NRC Canada

Fig. 2. Time course of posttranslational acetate label incorporation into alfalfa A2 histones. The specific radioactivity of histone peaks was determined in HPLC fractions and expressed as thousands of cpm per peak (filled symbols). The specific radioactivity in AUT gels, as shown in Fig. 1, was calculated from fluorography band intensity divided by Coomassie band intensity determined by quantitation of optical digital densitometry recordings (Waterborg et al. 1995). Fluorography exposures ranged from 2 to 30 days. An arbitrary scale was used to plot as open symbols the specific radioactivity of histones in AUT gels (AUT gel label). (A) Labeling of histone H3.1 (up triangles); (B) labeling of histone H3.2 (down triangles); (C) labeling of histone H4 (squares) and gel label of histone H2A (circles); (D) labeling of histone H2B (diamonds). Note that the amount of label in the two H3 variant peaks was similar, while the variant abundance differs twofold with twice as much H3.1 protein as H3.2 (Waterborg 1990).

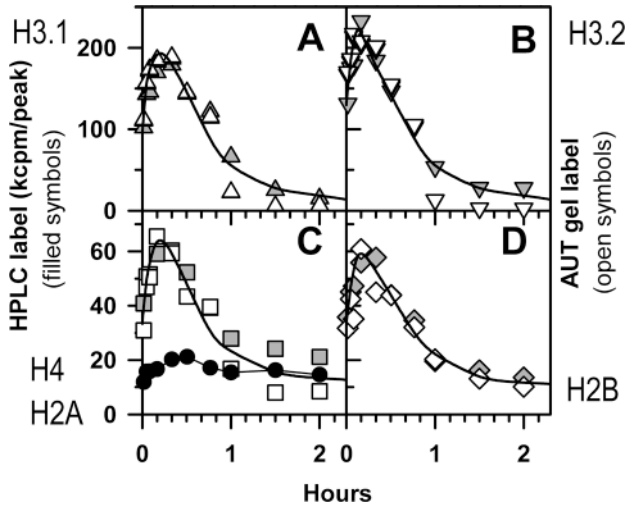

six lysines in the amino terminus of histone H2B can be acetylated (Fig. 1B). Sequence analysis of the histone H3 variants has shown that the six lysines in the amino terminus of each variant protein can be acetylated (Waterborg 1990). However, extensive irreversible lysine methylation in these histones (Waterborg 1990, 1993*b*) limits acetate labeling patterns typically to one level above that seen by Coomassie staining (Fig. 1, lane B).

In alfalfa cells with active synthesis of histones (Waterborg 1993*a*; Kapros et al. 1995), acetate labeling will include rapid cotranslational acetylation of the amino-terminal serine of histone H4 (Waterborg 1992*b*), resulting in labeling of nonacetylated H4. Subsequently, the rapid metabolism of acetate in plant cells (Waterborg et al. 1990) will create radioactive amino acids that will be stably incorporated into newly synthesized histones (Waterborg et al. 1990, 1995; Waterborg 1998, 2001). Thus, translation inhibitor cycloheximide was routinely used to limit acetylation labeling to posttranslational lysine acetylation.

The rapid metabolism of acetate becomes readily visible when alfalfa cells are incubated with a limited amount of tritiated acetate. When 0.5 mCi (1 mCi = 37 MBq) of tritiated acetate was added to 50 mL of growing A2 culture, the 4 μM acetate concentration was quickly exhausted, as revealed by the posttranslational labeling of histones (Fig. 2). In this non-steady-state labeling protocol, a transient maximum in the specific radioactivity of histones was observed at 10 min, followed by an apparently exponential decrease with a half-life of 30–45 min (Table 1). Label incorporation into histone H2A was low and slow and did not decay exponentially (Fig. 2C). Based on this result, the known multiplicity of overlapping histone H2A variants (Waterborg et al. 1987), and modification by phosphorylation (Waterborg et al. 1989), experimental analysis was restricted to histones H3.1, H3.2, H4, and H2B. The exponential character of the decrease in their labeling suggests that the radioactivity of the acetyl-CoA precursor pool for histone acetylation was diluted by new, unlabeled acetyl-CoA, while histone deacetylation and acetylation reactions continued, maintaining the steady-state acetylation level for all histones. If this dilution had been instantaneous, the observed half-life values (Table 1) would apply to dynamic, reversible histone deacetylation. As executed, this type of experiment will yield upper limit estimates for acetylation turnover rates. Although distinct half-life values were calculated for each of the major acetylation targets, the experimental error in this type of experiment was too large to distinguish significant differences in deacetylation rates.

Table 1. Turnover rates of posttranslational acetylation of histones in alfalfa A2 cells.

	Half-life (min)			
Histone	Pulse[a]	Pulse-chase[b]	Steady-state[c]	Average[d]
H3.1	44±22	53±7	22±6	35±13
H3.2	30±11	38±4	17±2	26±9
H4	38±10	42±9	19±4	30±11
H2B	35±13	32±11	23±3	28±5

[a]Accuracy of the estimates for the half-life values is represented by the standard error of the estimate (SigmaPlot) for a nonlinear regression fit representing an exponential decay of specific radioactivity. Estimates independently obtained from HPLC and AUT gel data for the exponential decay in specific radioactivity following labeling with 4 μM acetate (Fig. 2) were averaged, as were standard errors (SigmaPlot).

[b]Specific radioactivity data for a pulse-chase protocol (Fig. 3) were fitted to exponential decay analysis. Standard errors for half-life estimates are shown.

[c]Averaged standard error of estimate for a nonlinear regression fit representing an exponential increase to a maximum level of specific radioactivity. Estimates independently obtained from HPLC and AUT gel data for the exponential increase in specific radioactivity following labeling with 4 μM acetate of cultures in 0.2 mM acetate (Fig. 5) were averaged, as were standard errors.

[d]Best estimates of acetylation turnover rates based on the assumption that half-lives are overestimated by the pulse and pulse-chase protocols and underestimated by the steady-state protocols executed (see Discussion). The time difference with maximum and minimum values is given as standard error of the estimate.

Pulse-chase acetate labeling

A pulse-chase labeling protocol was developed in an attempt to reduce error rates and to refine estimates for histone acetylation turnover rates. Alfalfa cells were incubated with 4 μM tritiated acetate for 5 min. A 100-fold excess of ammonium acetate was added and cells were collected by centrifugation at 500 × *g* and resuspended in fresh MS growth medium supplemented with 0.4 mM ammonium acetate. The decay of acetate incorporated in the total histone extract, prior to HPLC fractionation, was exponential with a half-life of 38 ± 6 min. However, a third of the total label

© 2002 NRC Canada

Fig. 3. Analysis of the decay of acetate pulse-labeled histones during a chase period. The specific radioactivity (open symbols as used in Fig. 2) of histones (A) H3.1, (B) H3.2, (C) H4, and (D) H2B was determined in AUT gels following a 5-min incubation of alfalfa cells with 4 μM tritiated acetate and this value was set as 100%. The values determined throughout the chase period in 0.4 mM nonradioactive acetate were plotted relative to this starting value. The line represents a nonlinear regression fit representing an exponential decay of specific radioactivity. The dotted line represents the fraction of histone that apparently is stable. The average acetylation level per histone molecule, determined from radioactive fluorographs, is represented by solid symbols. A linear regression fit to these data is shown by a broken line, augmented by an error bar of the standard deviation of the mean for stable patterns.

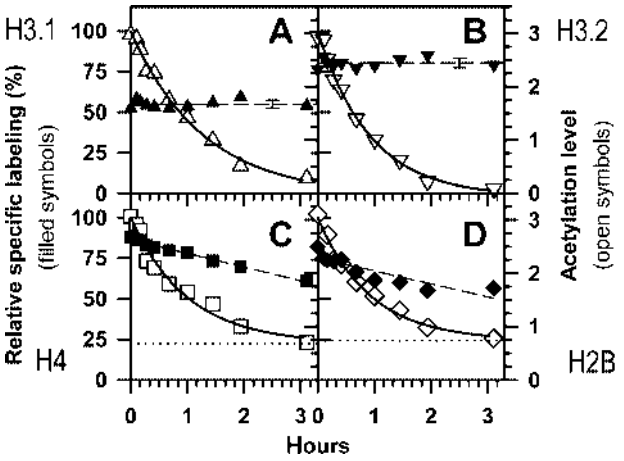

appeared stable (results not shown). Exponential decay of label in each histone was observed following AUT gel electrophoresis and fluorography (Fig. 3) and half-life rates were calculated (Table 1). These values were close to the upper limit estimates obtained by non-steady-state labeling and subject to less error. It appeared that deacetylation rates for histones H3.2 and H2B are faster than those for H3.1 and H4. Throughout the experiment, steady-state levels of histone acetylation did not change.

Inspection of the fluorography patterns during the chase (Fig. 1, lanes B–F) revealed a difference between the two H3 variants versus histones H4 and H2B. The relative abundance of the fluorography bands from mono- through tetraacetylation remained unchanged during the chase. This would be the result if the deacetylation rate for each level of H3 acetylation is the same. In contrast, the multiacetylated labeled forms of histones H4 and H2B disappear much faster from the fluorographs than mono- and diacetylated forms (Fig. 1). The relative distribution of label across the acetylation levels is quantitatively represented by a single value of the average number of radioactive acetylation of each histone (Waterborg et al. 1995; Waterborg 1998, 2000). This acetylation level value was constant throughout the experiment for histones H3.1 (Fig. 3A) and H3.2 (Fig. 3B). It decreased significantly in an apparently linear fashion for histones H4 (Fig. 3C) and H2B (Fig. 3D). This is consistent with a higher rate of deacetylation for multiacetylated H4 and H2B than for less modified forms and could also mark the existence of a stable form of acetate-labeled histone. The

Fig. 4. Assessment of steady-state conditions for acetate labeling of A2 cells. (A) Histones (symbols as used in Fig. 2) were labeled by 4 μM tritiated acetate in A2 cells grown for 30 min at 0.2 mM acetate and 10 μg cycloheximide/mL. The maximum labeling for each histone was set to 100%. The time axis is shown in log format to prevent data crowding. (B) Average acetylation level per histone molecule in A2 cells in growth medium with cycloheximide was determined by quantitation of Coomassie stained AUT gels (symbols as used in Fig. 2). (C) A 49-day AUT gel fluorograph. Lines mark each level of charge modification with numbers at the lowest, unlabeled, and highest levels of acetylation. Acetate labeling times were 2.5 min (lane A), 5 min (lane B), 10 min (lane C), 20 min (lane D), 41 min (lane E), 1.1 h (lane F), 1.8 h (lane G), 2.5 h (lane H), 3.3 h (lane I), 4 h (lane J), 5 h (lane K), 6 h (lane L), 7 h lane (M), 8.4 h (lane N), 9.3 h (lane O), and 10.4 h (lane P).

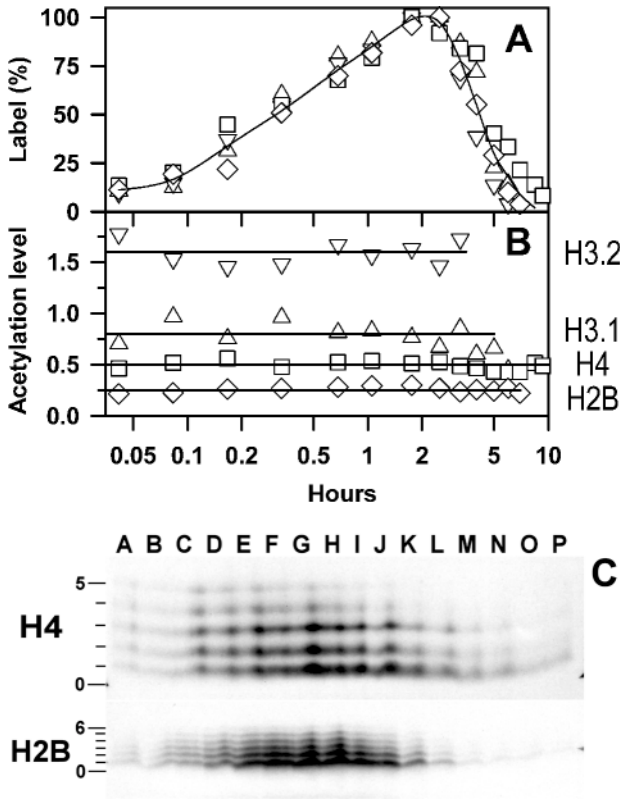

nonlinear regression analysis suggests that approximately 25% of the acetate pulse labeling of histones H4 (Fig. 3C) and H2B (Fig. 3D) is quite stable. This does not represent labeling of newly synthesized histones, as translation inhibitor cycloheximide limits acetate incorporation to post-translational processes.

Steady-state acetate labeling

One can measure rates of turnover from the pattern of increasing specific radioactivity if conditions are used that allow labeling under steady-state conditions (Waterborg 1998, 2001). Establishing steady-state conditions for the acetate-labeled pool of acetyl-CoA was attempted by preloading cells with unlabeled acetate for 30 min prior to the addition of 4 μM tritiated acetate. If 40 μM acetate was added to the culture medium, the labeling pattern with a maximum at

© 2002 NRC Canada

Fig. 5. Time course of posttranslational steady-state acetate labeling of alfalfa A2 histones. The specific radioactivity of histone peaks (filled symbols as used in Fig. 2) was determined in HPLC fractions and expressed as thousands of cpm per peak. The specific radioactivity of AUT gel label was calculated after 40-day fluorography of histone H3 and 49-day fluorography of H4 and H2B AUT gels (open symbols). An arbitrary but common scale of AUT gel labeling was used for all panels. The line represents a nonlinear regression fit representing an exponential increase of specific radioactivity to a steady-state maximum.

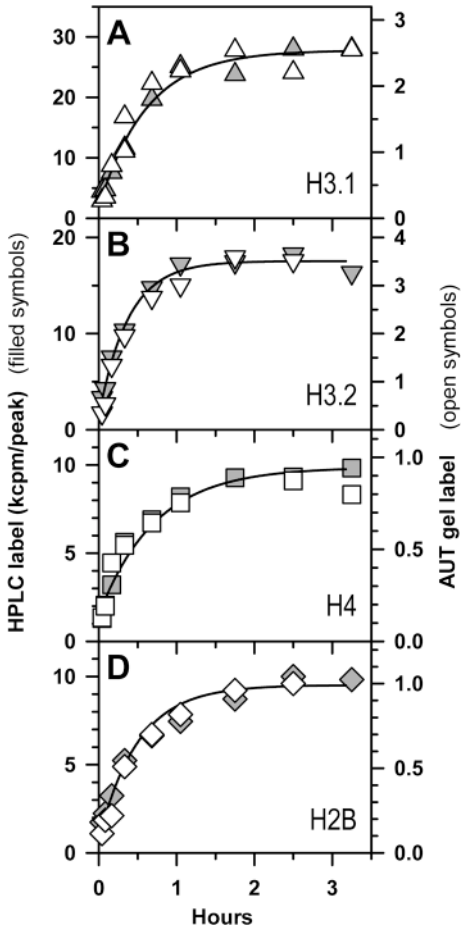

10 min after label addition (Fig. 2) was qualitatively the same, but two quantitative factors changed. A labeling maximum was observed 45 min after label addition (results not shown). The amount of label incorporated into histones decreased sharply, as expected from the dilution of the high specific activity tritiated acetate into the intracellular acetate pool that had been established over the preceding 30 min. Pretreatment with 200 or 500 μM acetate shifted the maximum to approximately 2.5 (Fig. 4A) and 5 h (results not shown) after label addition, respectively. The maximum amount of radioactivity incorporated into histones decreased further, requiring longer fluorography exposures to measure the specific radioactivity of histones. The choice was made to perform a detailed kinetic analysis using conditions of pretreatment with 200 μM acetate, since steady-state-like conditions were achieved for a period long enough to determine accurately the specific radioactivity of the histones at steady state if turnover rates determined by non-steady-state

Fig. 6. Dependence of steady-state specific radioactivity levels on the acetylation level of histones. The maximum, steady-state labeling of histones at each level of modification was derived from nonlinear regression analyses for histones (A) H3.1, (B) H3.2, (C) H4, and (D) H2B. Error bars represent standard errors of the estimates of the steady-state acetylation level (SigmaPlot). Each plot was scaled to the theoretical maximum where all acetyl groups are subject to turnover at the rates measured for each histone (Table 1). These theoretical unity values are depicted by the broken line plot.

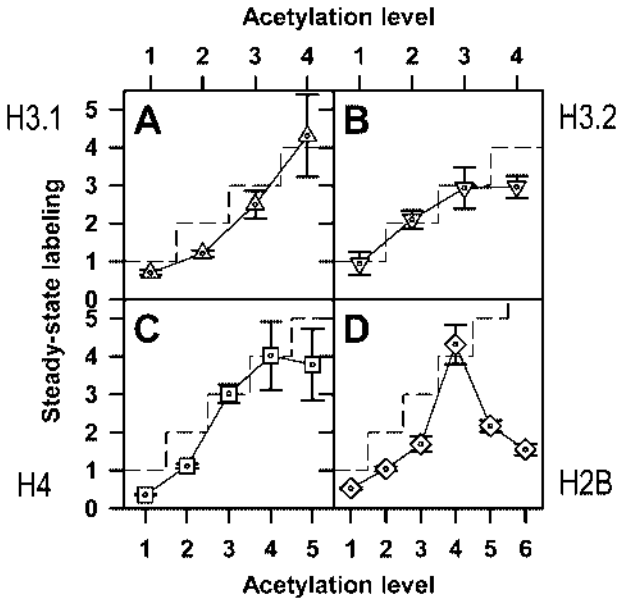

and pulse-chase experiments (Table 1) were valid. In preliminary experiments the accuracy of specific radioactivity measurements decreased as fluorography exposure times exceeded 100 days, as required following pretreatment with more than 200 μM acetate.

A critical requirement for acetate labeling by this approach is the need to limit acetate incorporation to posttranslational processes only. Cycloheximide added to a final concentration of 10 μg/mL in the growth medium prevented translational and cotranslational labeling of histones for more than 12 h, as judged by the complete absence of acetate incorporation into nonacetylated histone forms (results not shown). An additional experimental requirement, a constant level of histone acetylation, was maintained under experimental conditions for many hours (Fig. 4B).

The patterns of acetate incorporation over time fit well to the expected exponential rise in specific radioactivity for all histones analyzed (Fig. 5). A stable, maximum level of label incorporation was apparently achieved. A turnover rate of approximately 20 min was observed for all histones under these experimental conditions (Table 1). The differences that one can see between the patterns of label incorporation, e.g., a shorter time required for histone H3.2 to achieve a stable labeling maximum (Fig. 5B) than for histone H3.1 (Fig. 5A), were observed in every experiment. They were consistent with the differences observed in non-steady-state and pulse-chase experiments (Table 1). However, the accuracy of the turnover rates was insufficient to conclude that these differences are significant. The range of turnover rates

© 2002 NRC Canada

Fig. 7. Histone hyperacetylation by TSA. Histone acetylation levels, expressed as the average number of acetylated lysines per histone (A) H3.1, (B) H3.2, (C) H4, or (D) H2B, were measured in alfalfa A2 cells incubated for 2 h with TSA at the concentrations shown (open symbols as used in Fig. 2, solid line). Incorporation of tritiated acetate during the last 10 min of TSA treatment, preceded by 10 min by cycloheximide addition, was determined as the specific radioactivity in AUT gels. Label incorporation (filled symbols, broken line) was standardized by adjusting for the differing levels of steady-state acetylation in each histone and calculation of the label incorporation relative to the control cultures without TSA. Unlabeled ticks on the logarithmic *x*-axis denote 0.2 and 0.5 times the TSA concentration of the next higher labeled tick.

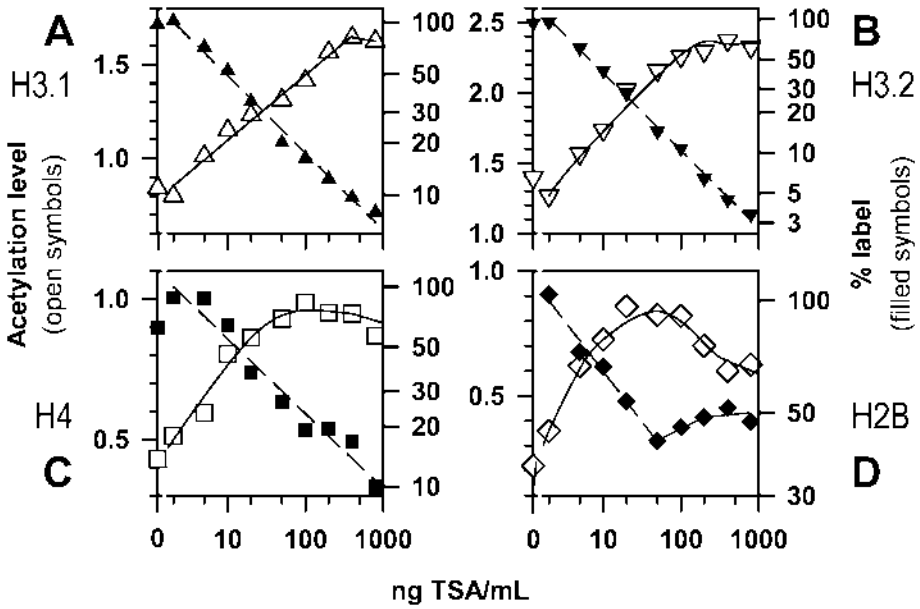

Fig. 8. Histone hyperacetylation patterns in alfalfa. Alfalfa cells were treated with 100 ng TSA/mL for 6 h (lanes B, D, F, H, and J) and the hyperacetylated histone pattern in Coomassie-stained AUT gels was compared with histone acetylation from control cells (lanes A, C, E, G, and I). Histone acetylation levels are indicated with numbers for lowest and highest levels of visible acetylation.

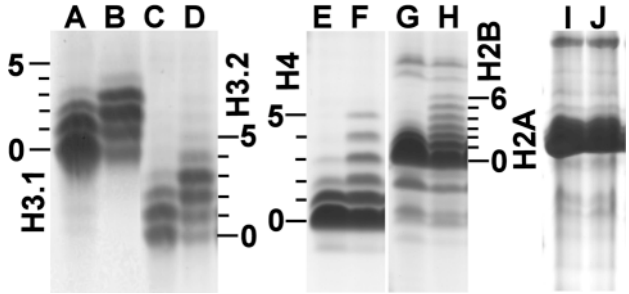

determined by this method should be considered minimum values. The decrease in histone labeling after 3 h (Fig. 4) clearly showed that a real steady-state condition was not achieved.

Analysis of histone acetylation turnover rates in *Chlamydomonas* (Waterborg 1998) and yeast (Waterborg 2001) by labeling to steady state revealed that turnover rates for defined levels of acetylation in H3 were the same as for total histone H3. In contrast, faster turnover was often observed for multiacetylated forms of histones H4 and H2B. Turnover rates were derived from specific radioactivity patterns in AUT gels for alfalfa histone H3.1 with one and two acetylated lysines and for histones H3.2, H4, and H2B with one to four modifications. With typical standard errors of 15–50%, significant rate differences were not detected for any level of acetylation relative to the turnover rate of total histone (results not shown). Visual inspection of acetate labeling (Fig. 4C) supports the notion that rates of acetylation at each modification level are the same.

One can estimate the extent to which acetyl-lysines are subject to acetyl turnover by determining the specific radioactivity reached at steady state for each modification level. If every acetyl group turns over at the same rate, the maximal specific radioactivity values would increase with the acetylation level by multiples of the label in monoacetylated histone. If the modification at some sites is relatively or completely stable, labeling would be low or absent at that site and an increase at values less than unity would result. Figure 6 shows the patterns in labeling levels for histone forms where maximal specific radioactivity values could be determined with fair accuracy and reproducibility through nonlinear regression analysis. Histone H3.2 results most closely approach the unity correlation between maximal steady-state labeling and acetylation level (Fig. 6B). This supports the notion derived from pulse-chase analysis (Fig. 3B) that all acetyl groups in histone H3, irrespective of the modification level, are subject to the turnover rates measured (Table 1). A fraction of histone H3.1 acetyl groups may be more stable than most (Fig. 6A), consistent with the marginally incomplete deacetylation seen in pulse-chase experiments (Fig. 3A). This suggests that deacetylation and reacetylation reactions engage histone forms with some level of acetylation, possibly at certain lysines. The existence of relatively stable acetylation sites is indicated by the low label in mono- and diacetylated forms of histones H4

© 2002 NRC Canada

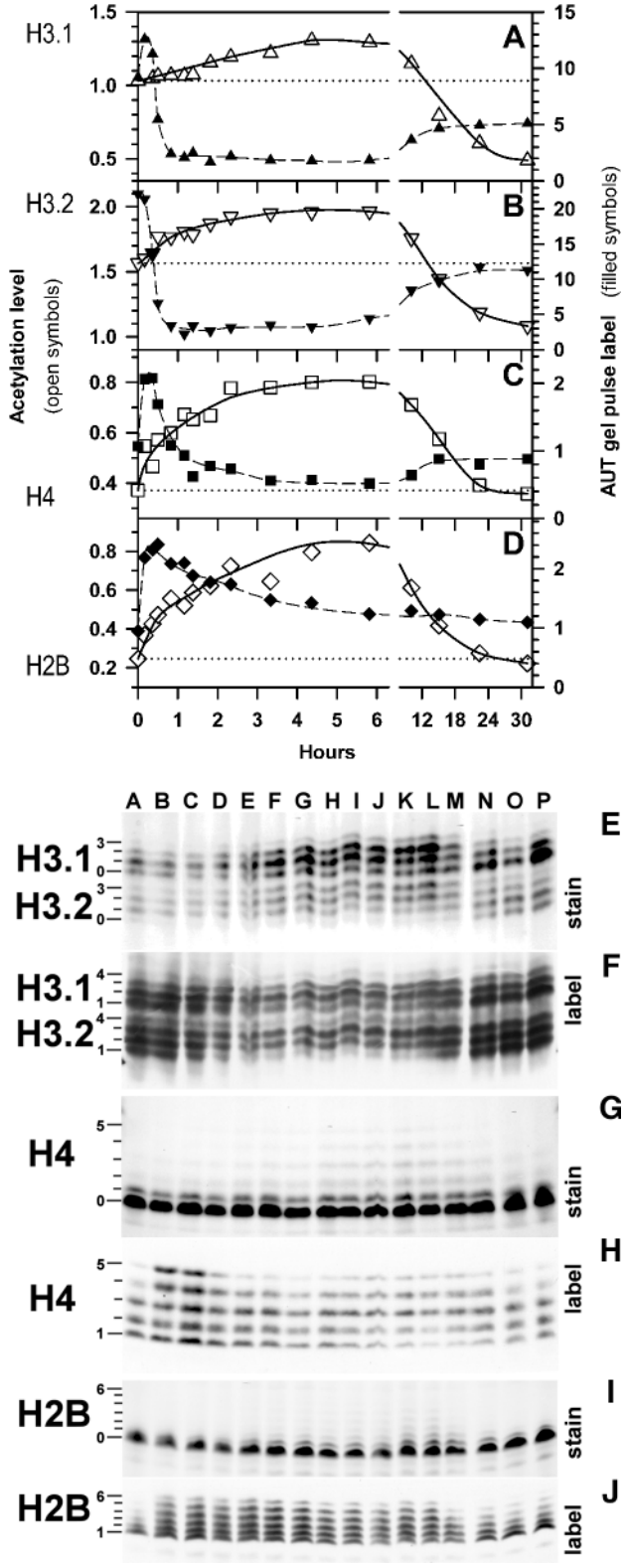

Fig. 9. Time dependence of histone steady-state acetylation and acetylation turnover in alfalfa A2 cells cultured with TSA. An A2 cell culture aliquot of 40 mL was supplied with cycloheximide (10 μg/mL). After 10 min, 0.5 mCi of tritiated acetate (to 4 μM) was added for 10 min and cells were collected as a sample for the 0-h time point. Histones (A, E, F) H3.1, (B, E, F) H3.2, (C, G, H) H4, and (D, I, J) H2B were prepared and analyzed in AUT gels. In parallel, identical aliquots were collected at defined times after addition of TSA to 100 ng/mL MS medium, having been incubated for the last 20 min with cycloheximide and for the last 10 min with tritiated acetate. The steady-state acetylation level, the average number of acetylated lysines per histone molecule, was plotted in Figs. 9A–9D as open symbols as used in Fig. 2. The line indicates the data pattern. A dotted line indicates the initial acetylation level above which hyperacetylation of histone is observed and below which hypoacetylation exists. AUT gels are shown as Coomassie-stained gel (stain, Figs. 9E, 9G, and 9I) and after fluorography for 5 days (label, Figs. 9F, 9H, and 9J). Histone acetylation bands are marked with the level of acetylation for lowest and highest visible bands shown. TSA treatment was for 0 min (lane A), 10 min (lane B), 22 min (lane C), 30 min (lane D), 50 min (lane E), 1.2 h (lane F), 1.4 h (lane G), 1.8 h (lane H), 2.3 h (lane I), 3.3 h (lane J), 4.4 h (lane K), 5.8 h (lane L), 10.1 h (lane M), 15.1 h (lane N), 22.5 h (lane O), and 31.1 h (lane P). The specific radioactivity of these samples was plotted using filled symbols in Figs. 9A–9D.

(Fig. 6C) and H2B (Fig. 6D) and was also detected in pulse-chase analyses (Figs. 3C and 3D). Inherently, any radioactivity incorporated posttranslationally will be subject to turnover at some rate when steady-state acetylation levels are stable (Fig. 4B), and complete loss of label over time was observed when experiments were continued long enough (Fig. 4A).

Induction of hyperacetylation by TSA

TSA has been shown to be an effective inhibitor of many HDACs, and treatment of cells in vivo has been shown to produce hyperacetylated histones. An exception to this rule has been yeast where many HDAC enzymes are effectively inhibited in vitro without the induction of hyperacetylation in vivo (Sanchez-del-Pino et al. 1994). It has been argued that this may be the result of the high level of histone acetylation, determined almost exclusively by dominant HAT activities (Waterborg 2001). The effect of TSA in alfalfa was studied to evaluate whether the balance between HAT and HDAC activities in vivo would be different for replacement histone H3.2, preferentially localized in highly acetylated, transcriptionally active chromatin, than for the generally distributed replicative histone H3.1 variant (Waterborg 1993*a*). These histones have identical amino-terminal sequences, offering identical substrate targets to modifying enzymes should the local chromatin conformation be the same. In addition, differences in the hyperacetylation response to TSA in histones H4 and H2B might clarify the kinetic differences with H3 histones.

TSA sensitivity of alfalfa was analyzed following treatment with TSA for 2 h by measuring the average number of acetylated lysines per histone. Effective hyperacetylation was observed at 100 ng TSA/mL (0.33 μM) in histones H3.1, H3.2, H4, and H2B (Fig. 7). The quantitative response was rather similar, producing roughly double the number of acetylated lysines per histone molecule. However, the qualitative response was very different. All histone H3 proteins,

© 2002 NRC Canada

Fig. 10. Changes in histone hyperacetylation upon repeated addition of TSA. Alfalfa histone acetylation levels, expressed as the average number of acetylated lysines per histone (A) H3.1, (B) H3.2, (C) H4, or (D) H2B, are shown in the upper panels. Incorporation of tritiated acetate during the last 10 min of TSA treatment, preceded by 10 min by cycloheximide addition, was determined as the specific radioactivity in AUT gels. These values, standardized on the steady-state acetylation level at the time of labeling and given as the percentage of labeling relative to the maximum level observed, are shown in the lower panels. The data set collected after a single addition of TSA to 100 ng/mL are shown by open symbols (as used in Fig. 2) and a solid line. Data collected after addition of a second aliquot of TSA after 4.2 h are shown by filled circles connected by a broken line. Data collected after addition of a second aliquot of TSA after 14.5 h are shown as shaded circles connected by a thin continuous line.

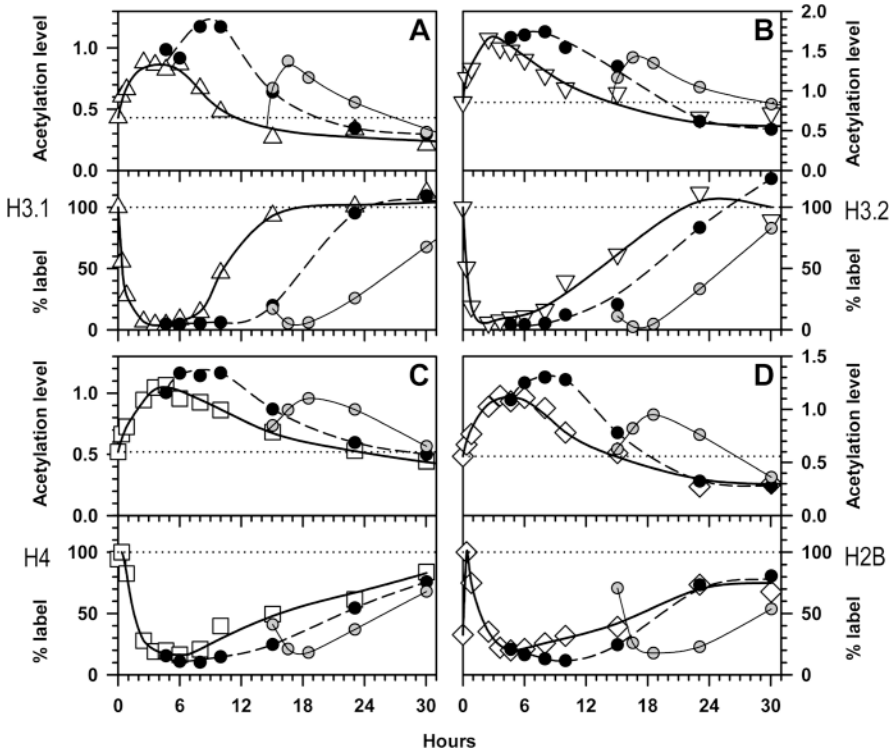

of both variants, appeared to increase acetylation level by one or two acetyl-lysines (Fig. 8, lanes A–D). In contrast, only a fraction of histone H4 and H2B molecules increased acetylation by several levels, while the rest remained unacetylated (Fig. 8, lanes E–H). The band pattern of histone H2A did not respond to TSA treatment (Fig. 8, lane J) and was excluded from further analysis.

Alfalfa cells respond within 10 min after addition of TSA by a detectable increase in the level of histone acetylation (Figs. 9A–9D). Acetylation levels increased for a period of 4–6 h following essentially an exponential response pattern with a half-life value of approximately 30 min. As in Fig. 8, a general shift in the acetylation distribution of the H3 histones was observed towards prominent triacetylated forms and a reduction in nonacetylated histone, especially for histone H3.2 (Fig. 9E). In contrast, only a limited fraction of histones H4 and H2B became hyperacetylated, gaining multiple acetylated lysines and allowing visualization of maximally modified pentaacetylated H4 (Fig. 9G) and hexaacetylated H2B forms (Fig. 9I).

The difference between the H3 variants versus histones H4 and H2B was further emphasized by the pattern of acetate labeling during the last 10 min of TSA treatment. This pulse-label protocol was chosen to see whether, or how much, turnover of histone acetylation existed after a period of inhibition of HDAC enzymes by TSA. As expected, labeling of the H3 variants was very high immediately following TSA addition (Figs. 9A and 9B), and the label distribution (Fig. 9F) was consistent with the existing steady-state pattern (Fig. 9E). This confirmed the impression that all histone H3 molecules were affected by the TSA treatment, all gaining acetyl-lysines that became labeled. After the initial spike of high labeling, acetate incorporation rapidly fell by at least a factor of 5 and stayed low (Figs. 9A and 9B). During this period of limited increase to the maximum of acetylation, the acetate labeling (Fig. 9F) remained representative of the steady-state acetylation pattern (Fig. 9E), indicating that the final increase in acetylation occurred across all histone H3 molecules. In contrast, high incorporation of acetate into histone H4 was delayed by 10 min, only reaching maximum values when steady-state acetylation had already increased (Fig. 9C). Gradually, acetate labeling decreased fourfold, while the acetylation labeling pattern (Fig. 9H) remained representative in its quantitative distribution of the fraction of H4 that became hyperacetylated rather than the total pattern of H4 acetylation (Fig. 9G). The same was true for histone H2B (Figs. 9I and 9J), except that the level of label incorporation remained very high and decreased only by 50% even when a maximum in H2B acetylation had been reached (Fig. 9D).

This difference between histones persisted even when the unexpected observation was made that after 6 h, histone

© 2002 NRC Canada

Fig. 11. Rate of hyperacetylation of alfalfa histone in TSA. The time required to reach maximum hyperacetylation following a single addition of TSA to 100 ng/mL or following a second addition of the same amount (Fig. 10) was determined for each individual level of acetylation of histones (A) H3.1 (up triangles) and H3.2 (down triangles) and (B) H4 (squares) and H2B (diamonds) by peak-fitting algorithms (SigmaPlot). The error bars give standard deviations for the three estimates. In Fig. 11A, the horizontal lines with raised and lowered error bars give the average and standard deviation for all estimates of H3.1 (solid line) and H3.2 (broken line), respectively. In Fig. 11B, the linear regression lines for H4 (solid line) and H2B (broken line) were calculated by SigmaPlot.

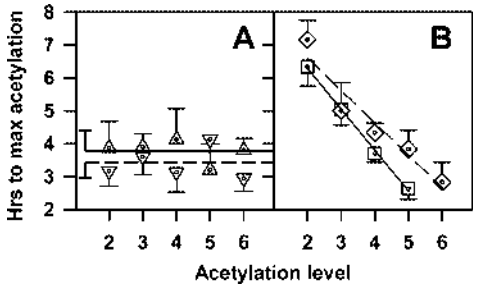

acetylation levels began to decrease, returning to starting values for histones H4 (Fig. 9C) and H2B (Fig. 9D) and even much lower for histone H3. Clearly, a condition of hypoacetylation, a steady-state level of acetylation lower than normal, was observed for histones H3.1 (Fig. 9A) and H3.2 (Fig. 9B). However, the relative acetylation levels of H3.1 and H3.2 retained their characteristic ratio of approximately 1:2 (Waterborg 1990, 1993*a*). Apparently the alfalfa cells did attempt to maintain higher acetylation levels, as deduced by a strong increase in acetylation labeling under these conditions (Fig. 9F). Such a response was not observed for H4 or H2B and acetylation turnover levels (Figs. 9C and 9D) and patterns (Figs. 9G–9J) for these histones returned to values observed in untreated cultures.

This experiment raised a number of questions that were pursued in subsequent tests. (*i*) Is TSA subject to metabolic inactivation or destruction in alfalfa cells so that effective HDAC inhibitor levels would gradually drop over a period of hours? One would expect that as steady-state acetylation levels become static due to HDAC inhibition by TSA, acetate incorporation should decrease to zero. This was not seen. Acetate labeling between 1 and 6 h in TSA remained quantitatively (Figs. 9A and 9B) and qualitatively (Fig. 9F) unchanged even when the increase in acetylation levels ceased (Figs. 9A, 9B, and 9E). Apparently, acetylation turnover persists and this might mean that cellular HDAC activities were incompletely inhibited. (*ii*) From the changes in acetate labeling for H4 (Fig. 9C) and H2B (Fig. 9D), one might deduce that inhibition of HDAC activities for these histones is quite limited. In fact, when acetylation levels decreased by half, acetate labeling changed only in pattern (Figs. 9H and 9J) but barely in level (Figs. 9C and 9D). Should one conclude that the spectrum of cellular HDAC activities for histones H2B and H4 is less sensitive to TSA inhibition than HDACs acting on histone H3? Differences in HDAC sensitivity to inhibitors like TSA have been observed in yeast and plants (Sanchez-del-Pino et al. 1994; Carmen et al. 1996, 1999; Lechner et al. 1996; Caretti et al. 1999). (*iii*) The observation of hypoacetylation in histone H3 raised the question whether cellular HDAC levels might have increased during the long treatment with TSA, as was deduced for human cells (DiRenzo et al. 2000), or whether HAT levels might have dropped, as has been reported for human cells (Covault et al. 1982) and maize (Lechner et al. 2000).

TSA is not stable in alfalfa cells

One can determine whether the effective concentration of an inhibitor decreases over time by addition of fresh inhibitor at different times during treatment. If the inhibitor is labile, subject to metabolic conversion or destruction, adding a fresh, equal aliquot should reestablish inhibition to a level higher than that observed after a single dose but less than after a single dose of twice the concentration. One would expect that inhibitor inactivation would continue to occur at the same rate. If cellular compensatory changes are induced by an inhibitor like TSA by an increase in HDAC activity (DiRenzo et al. 2000) and (or) a decrease in HAT activity (Lechner et al. 2000), one might see less than the level of inhibition observed after a single dose and possibly a faster loss of inhibition.

Hyperacetylation was induced in alfalfa cells by 100 ng TSA/mL, and maximal acetylation of histones H3.1, H3.2, H4, and H2B (Fig. 10) was observed in this experiment after approximately 4 h, followed by a gradual loss of acetylation resulting in 10–40% hypoacetylation by 30 h. After 4.2 h, the time that maximal hyperacetylation was reached, additional TSA was added to a parallel culture, increasing the nominal inhibitor concentration to 200 ng/mL. To a separate, parallel culture, TSA was added after 14.5 h to the same final concentration. All aliquots were labeled with acetate during the terminal 10 min of the treatment to allow assessment of residual rates of acetylation turnover. Histone steady-state acetylation levels (Fig. 10, upper panels) were compared with the specific radioactivity, standardized on the acetylation level as for Fig. 7 (Fig. 10, lower panels).

Addition of a second dose of TSA, given at a time that hyperacetylation was still high, increased hyperacetylation for all histones, and a maximum in this secondary acetylation was reached again after approximately 4 h (Fig. 10, upper panels). This is as predicted if the effective concentration of TSA is increased and if at least some net acetylation or acetylation turnover took place. The persistence of acetate incorporation, even if low (Fig. 10, lower panels), is consistent with the changes in steady-state acetylation observed. Although one might expect hyperacetylation to increase as much after the first aliquot of TSA, the nature of the HDAC–HAT balance determining the ultimate outcome does not necessarily result in a linear response.

Addition of a second dose of TSA at a time when much of the initial hyperacetylation had been lost allowed a more quantitative analysis. With nearly normal acetylation levels restored (Fig. 10, upper panels), addition of a new and equal aliquot of TSA should result in hyperacetylation as rapid and extensive as that observed after the initial addition of TSA. Hyperacetylation clearly was induced again, supporting the notion that TSA had been inactivated or removed. The time required to reach maximal hyperacetylation was,

© 2002 NRC Canada

within experimental limits, identical to the initial one. This suggests that the rate of TSA inactivation had not changed. However, the maximum of hyperacetylation the second time was clearly and consistently lower (Fig. 10, upper panels). This demonstrates that the cellular balance between residual HDAC activity and HAT activity had shifted between 4 and 18 h after the initial TSA addition to be more dominated by deacetylation reactions. Thus, over the subsequent 12 h in TSA the balance continued to shift further towards HDAC dominance and the rate of loss of hyperacetylation increased. The limited number of data points collected and the variations among data for different histones made it difficult to quantify this. Indirectly measured as increased acetate incorporation into hypoacetylated histones by the end of the experiment, the net level of cellular HDAC activity had clearly exceeded initial levels (Fig. 10, lower panels). In conclusion, addition of TSA to alfalfa cells results in histone hyperacetylation, TSA inactivation, induction of HDAC activities, and histone hypoacetylation.

Detailed analysis showed that the time required to reach maximal hyperacetylation differed slightly among histone species (Fig. 10) as did the acetylation level in some histones. Hyperacetylation rates were independent of the acetylation level in histones H3.1 and H3.2 (Fig. 11A). It appears that TSA-induced hyperacetylation of histone H3.2 was somewhat faster than for histone H3.1. A similar difference was observed for the acetylation turnover rate in the absence of TSA (Table 1). Significant differences in the rate of TSA-induced hyperacetylation were observed for the distinct acetylated forms of histone H4 and H2B (Fig. 11B). TSA inhibition of deacetylation lead to a rapid accumulation of multiacetylated forms of histone H4 and H2B and the accumulation rate for the less acetylated forms was much lower. This type of difference has been observed before in the absence of TSA for acetylation turnover rates of histones H4 and H2B in *Chlamydomonas* (Waterborg 1998) and in yeast (Waterborg 2001). The significant differences among hyperacetylation rates in TSA (Fig. 11B) suggested that differences in the rates of acetylation turnover in the absence of TSA might exist among acetylation levels of H4 and H2B, but attempts to prove this failed due to experimental limits (see above).

Inhibition of histone acetylation turnover by TSA

The apparent degree of inhibition of HDAC activity in vivo shown in Fig. 9, as measured by acetate labeling during the terminal 10 min of TSA treatment, is not a valid, quantitative measure. Over time, the amount of acetylated lysines and thus the amount of substrate for HDAC action increases (Fig. 9). A standard TSA treatment time of 2 h was chosen to measure more accurately the degree of HDAC inhibition in vivo. After 2 h in TSA, four to six half-lives of acetylation turnover (Table 1), hyperacetylation had been established but had yet to reach steady-state levels (Fig. 11). Residual HDAC activity was measured by acetate incorporation during the last 10 min of TSA treatment. The specific activity of label was plotted in a way to correct for the existing level of histone acetylation, i.e., the concentration of substrate for HDAC action. Complete inhibition was observed for HDAC activities acting on histones H3.1, H3.2, and H4 whereas inhibition of HDACs acting on histone H2B was maximally 60% and insensitive to increasing concentrations of TSA (Fig. 7). This result is consistent with the limited reduction in acetate labeling when hyperacetylation has become established (Fig. 9D). However, these results do not prove that HDACs acting on histone H2B would display the same pattern of inhibition by TSA in vitro. The constant pattern of mono- through hexaacetylation labeling of histone H2B (Fig. 9J, lanes C–L) could represent HAT acetylation with little or no deacetylation by HDAC activities. The results shown in Fig. 10 give support to this notion. When acetate label incorporation is plotted in the same way as in Fig. 7 (Fig. 10, lower panels), residual acetylation levels were 5% for histones H3 (Figs. 10A and 10B), 10% for H4 (Fig. 10C), and 15% for H2B (Fig. 10D). These values were measured under the steady-state conditions of stable hyperacetylation. In contrast, measurements reported in Fig. 7D were obtained after 2 h in TSA when acetylation levels are still rising (Figs. 9 and 10). Thus, it is likely that HDAC activity toward histone H2B is inhibited by TSA nearly as well as for the other histones. The residual 40% acetylation rate at high TSA concentrations in this experiment (Fig. 7D) represents HAT-dependent net acetylation and does not reflect HDAC-dependent acetylation turnover.

Discussion

Histone acetylation turnover

This paper presents the first estimates of the rates of histone acetylation and deacetylation for a plant species. Three different experimental approaches were used to measure the turnover of acetyl groups on the lysines located in the amino termini of alfalfa core histones. In the first method, a pulse-label protocol, the pattern of posttranslational label incorporation reveals the rapid exhaustion of the label in the cell pool (Fig. 2) with deacetylation rates of 30–45 min (Table 1). These represent upper limit values, as the intracellular production of unlabeled acetyl-CoA would decrease the specific radioactivity of the pool only gradually. The pulse-chase experiments (Fig. 3) attempted to create a more effective chase by addition of a 100-fold excess of unlabeled acetate. One cannot chase directly with unlabeled acetyl-CoA because it cannot enter through the cell membrane. The deacetylation rates, i.e., acetylation turnover rates given a stable acetylation level of histones, were the same as in the non-steady-state pulse-label protocol (Table 1). Thus, entry of added acetate into the acetyl-CoA pool appears to be rate limiting.

A third experimental design, labeling to steady state, was used to assess the validity of the prior, maximum rates of acetylation turnover. Preloading of alfalfa cells with 200 μM acetate, prior to the addition of label, only transiently achieved steady-state conditions (Fig. 4). Within the accuracy of specific radioactivity of histones in HPLC fractions and AUT gels, a mathematically valid steady-state condition was reached (Fig. 5). Under conditions of stable histone acetylation levels (Fig. 4B), the experimental rates of acetylation are measures of acetylation turnover (Table 1). In view of the quasi-steady-state condition reached, the half-life values of 17–23 min (Table 1) must be considered minimum estimates. Averaging of maximum pulse and pulse-

© 2002 NRC Canada

chase values with minimum steady-state rates, with a clear indication of data accuracy, produces the best current estimate for histone acetylation turnover in plants (Table 1).

It is likely that the rate of turnover in replacement histone variant H3.2, more highly acetylated through its preferential assembly into transcriptionally active chromatin (Waterborg 1993*a*), is faster than in replication variant H3.1 (Table 1). In every experimental design, the half-life for acetylation turnover in H3.2 was, on average, 72 ± 4% of that measured for histone H3.1 (Table 1). The time to maximal hyperacetylation for histone H3.2 was less than that for H3.1 (Fig. 11). However, in no experiment was the difference statistically significant. Taking into account the relative abundance of the two variant forms, the average acetylation turnover rate for histone H3 was in every experiment very close to the estimates obtained for histones H4 and H2B. Thus, in general, histone acetylation turnover rates vary little, if at all, among core histone variants in alfalfa and have a half-life of about 0.5 h.

Histone hyperacetylation occurs when deacetylation rates are reduced by HDAC inhibition by inhibitors like TSA, while acetylation by HAT enzymes continues, until a new equilibrium has been reached. Effective inhibition of HDACs in alfalfa was established by 100 ng TSA/mL (Fig. 7). The rate of hyperacetylation is a combination of rate of acetylation and residual rate of deacetylation. Similar to the best estimates for acetylation turnover (Table 1), the hyperacetylation half-life was also about 0.5 h (Figs. 9 and 10). Thus, inducing artificially high levels of histone acetylation does not appear to change the kinetics of acetylation turnover. The rate at which changes in gene expression occur in plants is consistent with the dynamics of histone acetylation reported. Genes may be activated through external stimuli over a period of minutes to hours, and, based on experiments in yeast (Kuo et al. 1998), this requires in many cases increased histone acetylation at gene promoters and across activated gene sequences (Wittschieben et al. 1999; Brown et al. 2000). Also, it is now well established that gene silencing can be induced through DNA methylation, association with HDACs, and loss of chromatin acetylation (Wade et al. 1998), again a process that takes many minutes or hours. Thus the rates of acetylation turnover measured in alfalfa are consistent with the rates at which genes in plants are activated or silenced through modulation of chromatin acetylation.

Histone acetylation in H4 and H2B fundamentally differs from acetylation in H3

Study of the dynamics of histone acetylation in *Chlamydomonas* (Waterborg 1998) and yeast (Waterborg 2001) has shown that acetylation of histone H3 is different from acetylation of histones H4 and H2B. Experiments described here support these differences and suggest that they represent fundamentally different patterns.

The rate of histone acetylation turnover of histone H3 is the same for each level of acetylation. This was observed for both H3 variants in alfalfa (Figs. 1 and 3) and for histone H3 in *Chlamydomonas* (Waterborg 1998) and yeast (Waterborg 2001). Similarly, the rate of hyperacetylation of H3 was not dependent on the level of acetylation in alfalfa (Fig. 11) and *Chlamydomonas* (Waterborg 1998). The specific radioactivity values reached by each level of acetylation in histone H3 at steady state (Fig. 6) suggests that virtually every histone H3 molecule is a substrate for both enzymes. The same conclusion was reached for yeast (Waterborg 2001) and *Chlamydomonas* for every histone H3 molecule that could be hyperacetylated by TSA (Waterborg 1998). Apparently, HDAC and HAT enzymes act on lysines within the amino terminus of histone H3 irrespective of the state of acetylation of any of the other lysines. This is consistent with prior observations in alfalfa (Waterborg 1990) and *Chlamydomonas* (Waterborg et al. 1995) that histone acetylation of histone H3 lacks site specificity. However, this does not exclude the possibility that other modifications within the amino terminus of histone H3 affect acetylation. The interdependence of acetylation of lysine 14 and phosphorylation of serine 10 has been demonstrated in animal cells (Barratt et al. 1994; Cheung et al. 2000; Clayton et al. 2000; Lo et al. 2000). Irreversible methylation of lysines 4, 9, and 27 in histone H3 of alfalfa (Waterborg 1990, 1993*b*) and *Chlamydomonas* (Waterborg et al. 1995) clearly limits acetylation, and lysine methylation of histone H3 in *Chlamydomonas* limited TSA-induced hyperacetylation to pentaacetylation (Waterborg 1998). In the past, we have described that acetylation of both histone H3 variants was limited by lysine methylation (Waterborg 1990). This study clearly illustrates this limit again in the pattern of hyperacetylation of both histone H3 variants. Triacetylated forms accumulate as the most abundant form (Figs. 8 and 9E) and as the form most intensely labeled by acetate (Fig. 9F).

The differences between histone H4 or H2B with histone H3 are most clearly demonstrated by the pattern of TSA-induced hyperacetylation (Fig. 8). Hyperacetylation of both histones is limited to a subset of molecules that are very rapidly labeled to penta- or hexaacetylated levels by acetate (Figs. 9G and 9I). Based on the acetylation patterns, the fraction of molecules hyperacetylated in TSA is the same as the molecules that are rapidly pulse labeled by acetate in the absence of TSA (Fig. 1). Analysis of maximal levels of specific radioactivity attained upon steady-state labeling confirms that fast acetylation turnover is limited to a subset of histone H4 (Fig. 6C) and H2B molecules (Fig. 6D). A similar conclusion was reached for *Chlamydomonas* (Waterborg 1998) and yeast (Waterborg 2001).

The preferential loss of acetylation labeling of multiacetylated forms of histones H4 and H2B during a chase period (Fig. 1), quantifiable as a decrease in radioactive acetylation level (Figs. 3C and 3D), and during the latter stages of labeling experiments (Fig. 4C, lanes I–P) suggests a higher rate of turnover for acetyl groups in multiacetylated molecules. This has been demonstrated in *Chlamydomonas* (Waterborg 1998) and yeast (Waterborg 2001). We failed to detect rate differences for acetylation turnover in alfalfa. However, indirect evidence was obtained in experiments with TSA that higher rates of acetylation exist in multiacetylated H4 and H2B, and the rate to maximal hyperacetylation clearly reveals differences in acetylation levels that do not exist in histone H3 (Fig. 11).

The differences deduced between acetylation of H3 histones with acetylation of histones H4 and H2B may reflect a fundamentally distinct role, based on the differences of lo-

© 2002 NRC Canada

calization of the histones within the nucleosomes (Luger et al. 1997). The amino termini of histone H3 appear to be functionally involved in the compaction of the chromatin fiber, assisting or cooperating with linker histones (Leuba et al. 1998*a*, 1998*b*). In contrast, the other amino termini are more likely involved in internucleosome binding based on chromatin fiber changes upon proteolysis or hyperacetylation (Allan et al. 1982; Garcia-Ramirez et al. 1995; Carruthers and Hansen 2000), which may be reflected in the binding of H4 termini across nucleosomes within crystals (Luger et al. 1997).

Effects of TSA in vivo

TSA is apparently an effective inhibitor of cellular HDACs in alfalfa as judged by the concentration-dependent decrease in acetate labeling during the terminal 10 min of a 2-h treatment (Fig. 7). The initial impression that inhibition of HDACs acting on histone H2B might be less than complete (Fig. 7D) was proven false when terminal acetate labeling was corrected for existing acetylation levels and was measured at constant acetylation levels (Fig. 10D). Thus, the apparent limit of 60% inhibition of H2B acetylation (Fig. 7D) was only seen when hyperacetylation levels continued to increase and acetate labeling marked net acetylation rather than HDAC-dependent acetylation turnover. Overall, inhibition of HDAC activities in alfalfa by TSA was at least 85% for all histones (Figs. 7 and 10), and no indication was found that in alfalfa, HDAC activities might exist that are insensitive to inhibition by TSA, as observed for yeast and maize (Sanchez-del-Pino et al. 1994; Carmen et al. 1996, 1999; Lechner et al. 1996; Caretti et al. 1999).

TSA addition experiments demonstrated that the effective level of HDAC inhibitor decreased over time (Fig. 10), but whether this is due to metabolic destruction or through removal by another process is unknown. In the past, we have demonstrated that *n*-butyrate, another commonly used inhibitor of HDACs, cannot be used in alfalfa to induce hyperacetylation because it is readily metabolized through acetyl-CoA (Waterborg et al. 1990). Transient hyperacetylation has been described before in human tissue culture (Siavoshian et al. 2000). Inhibition of cell proliferation by TSA in pea root meristems, measured by changes in the mitotic index, disappears within 12 h (Murphy et al. 2000). We have observed that TSA addition to alfalfa cells in culture causes a lag in the increase of cell mass that lasts for a number of hours and that cell proliferation ultimately resumes.

Histone hypoacetylation has been described for mammalian cells in culture when *n*-butyrate was removed from the culture medium (Covault et al. 1982). This result was attributed to down-regulation of cellular HAT activity based on the observation that deacetylation rates under hypoacetylation conditions were the same as in untreated culture, while acetylation rates had decreased. In maize, down-regulation of HAT activity has been observed (Lechner et al. 2000). However, the HAT was identified as cytoplasmic HAT B, responsible for diacetylation of newly synthesized histone H4. Its down-regulation following treatment of maize with HC toxin, a natural fungal HDAC inhibitor, could be related to the interruption of cell proliferation and cessation of histone synthesis. Our observations in alfalfa suggest that TSA induces overexpression of HDAC without a detectable effect on HAT levels. Addition of a second aliquot of TSA by the time that hyperacetylation has decreased to near normal levels leads to renewed hyperacetylation at the net rate of acetylation that was observed after the initial addition of TSA (Fig. 10). However, the maximal level of hyperacetylation induced upon readdition is lower, indicative of an increase in HDAC activity relative to HAT levels over the 14 h between the first and second maxima of hyperacetylation (Fig. 10). The increased level of cellular HDAC activity is responsible for the drop in steady-state acetylation levels into hypoacetylation, observed consistently but with varying magnitudes after addition of a single or double dose of TSA (Figs. 9 and 10). Apparently the cells try to maintain histone acetylation levels within boundaries that are exceeded during TSA treatment. It can respond by increasing HDAC levels, as seen in human cells in the induction of HDAC-1 overexpression (DiRenzo et al. 2000). Thus the use of TSA in long-term experiments with the aim to change gene expression directly through histone acetylation or indirectly through changes in DNA methylation (Selker 1998) may lead to unexpected and unintended consequences.

Acknowledgements

Part of this work was supported by National Science Foundation grant DCB 9118999 to J.H.W. We gratefully acknowledge the research opportunities created by Dr. M. Martinez-Carrion. We thank Dr. W.T. Morgan for his careful reading of the manuscript.

References

Ahringer, J. 2000. NuRD and SIN3, histone deacetylase complexes in development. Trends Genet. **16**: 351–356.

Allan, J., Harborne, N., Rau, D.C., and Gould, H. 1982. Participation of core histone 'tails' in the stabilization of the chromatin solenoid. J. Cell Biol. **93**: 285–297.

Allfrey, V.G. 1977. Post-synthetic modifications of histone structure: a mechanism for the control of chromosome structure by the modulation of histone–DNA interactions. *In* Chromatin and chromosome structure. *Edited by* H.J. Li and R.A. Eckhardt. Academic Press, New York. pp. 167–191.

Arfmann, H.A., and Haase, E. 1981. Effect of sodium butyrate on the modification of histones in cell cultures of *Nicotiana tabacum* cultivar white-burley. Plant Sci. Lett. **21**: 317–324.

Ayer, D.E. 1999. Histone deacetylases: transcriptional repression with SINers and NuRDs. Trends Cell Biol. **9**: 193–198.

Barratt, M.J., Hazzalin, C.A., Cano, E., and Mahadevan, L.C. 1994. Mitogen-stimulated phosphorylation of histone H3 is targeted to a small hyperacetylation-sensitive fraction. Proc. Natl. Acad. Sci. U.S.A. **91**: 4781–4785.

Belyaev, N.D., Houben, A., Baranczewski, P., and Schubert, I. 1997. Histone H4 acetylation in plant heterochromatin is altered during the cell cycle. Chromosoma, **106**: 193–198.

Belyaev, N.D., Houben, A., Baranczewski, P., and Schubert, I. 1998. The acetylation patterns of histones H3 and H4 along *Vicia faba* chromosomes are different. Chromosome Res. **6**: 59–64.

Bird, A.P., and Wolffe, A.P. 1999. Methylation-induced repression — belts, braces and chromatin. Cell, **99**: 451–454.

© 2002 NRC Canada

Brosch, G., Ransom, R., Lechner, T., Walton, J.D., and Loidl, P. 1995. Inhibition of maize histone deacetylases by HC toxin, the host-selective toxin of *Cochliobolus carbonum*. Plant Cell, **7**: 1941–1950.

Brown, C.E., Lechner, T., Howe, L., and Workman, J.L. 2000. The many HATs of transcription coactivators. Trends Biochem. Sci. **25**: 15–19.

Buzek, J., Riha, K., Siroky, J., Ebert, I., Greilhuber, J., and Vyskot, B. 1998. Histone H4 underacetylation in plant facultative heterochromatin. Biol. Chem. **379**: 1235–1241.

Caretti, G., Motta, M.C., and Mantovani, R. 1999. NF-Y associates with H3–H4 tetramers and octamers by multiple mechanisms. Mol. Cell. Biol. **19**: 8591–8603.

Carmen, A.A., Rundlett, S.E., and Grunstein, M. 1996. HDA1 and HDA3 are components of a yeast histone deacetylase (HDA) complex. J. Biol. Chem. **271**: 15 837 – 15 844.

Carmen, A.A., Griffin, P.R., Calaycay, J.R., Rundlett, S.E., Suka, Y., and Grunstein, M. 1999. Yeast HOS3 forms a novel trichostatin A-insensitive homodimer with intrinsic histone deacetylase activity. Proc. Natl. Acad. Sci. U.S.A. **96**: 12 356 – 12 361.

Carruthers, L.M., and Hansen, J.C. 2000. The core histone N-termini function independently of linker histones during chromatin condensation. J. Biol. Chem. **275**: 37 285 – 37 290.

Chestier, A., and Yaniv, M. 1979. Rapid turnover of acetyl groups in the four core histones of simian virus 40 minichromosomes. Proc. Natl. Acad. Sci. U.S.A. **76**: 46–50.

Cheung, P., Tanner, K.G., Cheung, W.L., Sassone-Corsi, P., Denu, J.M., and Allis, C.D. 2000. Synergistic coupling of histone H3 phosphorylation and acetylation in response to epidermal growth factor stimulation. Mol. Cell. **5**: 905–915.

Clayton, A.L., Rose, S., Barratt, M.J., and Mahadevan, L.C. 2000. Phosphoacetylation of histone H3 on c-fos- and c-jun-associated nucleosomes upon gene activation. EMBO J. **19**: 3714–3726.

Covault, J., Sealy, L., Schnell, R., Shires, A., and Chalkley, R. 1982. Histone hypoacetylation following release of HTC cells from butyrate. J. Biol. Chem. **257**: 5809–5815.

Dhalluin, C., Carlson, J.E., Zeng, L., He, C., Aggarwal, A.K., and Zhou, M.M. 1999. Structure and ligand of a histone acetyltransferase bromodomain. Nature (Lond.), **399**: 491–496.

DiRenzo, J., Shang, Y., Phelan, M., Sif, S., Myers, M., Kingston, R., and Brown, M. 2000. BRG-1 is recruited to estrogen-responsive promoters and cooperates with factors involved in histone acetylation. Mol. Cell. Biol. **20**: 7541–7549.

Doetzlhofer, A., Rotheneder, H., Lagger, G., Koranda, M., Kurtev, V., Brosch, G., Wintersberger, E., and Seiser, C. 1999. Histone deacetylase 1 can repress transcription by binding to Sp1. Mol. Cell. Biol. **19**: 5504–5511.

Fax, P., Lehmkueler, O., Kuehn, C., Esche, H., and Brockmann, D. 2000. E1A(12)S-mediated activation of the Adenovirus type 12 E2 promoter depends on the histone acetyltransferase activity of p300/CBP. J. Biol. Chem. **275**: 40 554 – 40 560.

Garcia-Ramirez, M., Rocchini, C., and Ausio, J. 1995. Modulation of chromatin folding by histone acetylation. J. Biol. Chem. **270**: 17 923 – 17 928.

Gilbert, S.L., and Sharp, P.A. 1999. Promoter-specific hypoacetylation of X-inactivated genes. Proc. Natl. Acad. Sci. U.S.A. **96**: 13 825 – 13 830.

Hebbes, T.R., and Allen, S.C.H. 2000. Multiple histone acetyltransferases are associated with a chicken erythrocyte chromatin fraction enriched in active genes. J. Biol. Chem. **275**: 31 347 – 31 352.

Hecht, A., Vleminckx, K., Stemmler, M.P., van Roy, F., and Kemler, R. 2000. The p300/CBP acetyltransferases function as transcriptional coactivators for beta-catenin in vertebrates. EMBO J. **19**: 1839–1850.

Hendzel, M.J., and Davie, J.R. 1991. Dynamically acetylated histones of chicken erythrocytes are selectively methylated. Biochem. J. **273**: 753–758.

Idei, S., Kondo, K., Turner, B.M., and Fukui, K. 1996. Tomographic distribution of acetylated histone H4 in plant chromosomes, nuclei and nucleoli. Chromosoma, **105**: 293–302.

Jackson, V., Shires, A., Chalkley, R., and Granner, D.K. 1975. Studies on highly metabolically active acetylation and phosphorylation of histones. J. Biol. Chem. **250**: 4856–4863.

Jacobson, R.H., Ladurner, A.G., King, D.S., and Tjian, R. 2000. Structure and function of a human TAF(II)250 double bromodomain module. Science (Washington, D.C.), **288**: 1422–1425.

Kadosh, D., and Struhl, K. 1997. Repression by Ume6 involves recruitment of a complex containing Sin3 corepressor and Rpd3 histone deacetylase to target promoters. Cell, **89**: 365–372.

Kapros, T., Robertson, A.J., and Waterborg, J.H. 1995. Histone H3 transcript stability in alfalfa. Plant Mol. Biol. **28**: 901–914.

Kuo, M.H., Zhou, J.X., Jambeck, P., Churchill, M.E.A., and Allis, C.D. 1998. Histone acetyltransferase activity of yeast Gcn5p is required for the activation of target genes in vivo. Genes Dev. **12**: 627–639.

Kurooka, H., and Honjo, T. 2000. Functional interaction between the mouse Notch1 intracellular region and histone acetyltransferases PCAF and GCN5. J. Biol. Chem. **275**: 17 211 – 17 220.

Lechner, T., Lusser, A., Brosch, G., Eberharter, A., Goralik-Schramel, M., and Loidl, P. 1996. A comparative study of histone deacetylases of plant, fungal and vertebrate cells. Biochim. Biophys. Acta, **1296**: 181–188.

Lechner, T., Lusser, A., Pipal, A., Brosch, G., Loidl, A., Goralik-Schramel, M., Senfra, R., Wegener, S., Walton, J.D., and Loidl, P. 2000. RPD3-type histone deacetylases in maize embryos. Biochemistry, **39**: 1683–1692.

Leuba, S.H., Bustamante, C., Zlatanova, J., and Van Holde, K. 1998*a*. Contributions of linker histones and histone H3 to chromatin structure: scanning force microscopy studies on trypsinized fibers. Biophys. J. **74**: 2823–2829.

Leuba, S.H., Bustamante, C., Van Holde, K., and Zlatanova, J. 1998*b*. Linker histone tails and N-tails of histone H3 are redundant: scanning force microscopy studies and reconstituted fibers. Biophys. J. **74**: 2830–2839.

Lo, W.S., Trievel, R.C., Rojas, J.R., Duggan, L., Hsu, J.Y., Allis, C.D., Marmorstein, R., and Berger, S.L. 2000. Phosphorylation of serine 10 in histone H3 is functionally linked in vitro and in vivo to Gcn5-mediated acetylation at lysine 14. Mol. Cell. **5**: 917–926.

Luger, K., Mäder, A.W., Richmond, R.K., Sargent, D.F., and Richmond, T.J. 1997. Crystal structure of the nucleosome core particle at 2.8Å resolution. Nature (Lond.), **389**: 251–260.

Lusser, A., Kolle, D., and Loidl, P. 2001. Histone acetylation: lessons from the plant kingdom. Trends Plant Sci. **6**: 59–65.

Matangkasombut, O., Buratowski, R.M., Swilling, N.W., and Buratowski, S. 2000. Bromodomain factor 1 corresponds to a missing piece of yeast TFIID. Genes Dev. **14**: 951–962.

Mizzen, C.A., and Allis, C.D. 2000. New insights into an old modification. Science (Washington, D.C.), **289**: 2290.

Murphy, J.P., McAleer, J.P., Uglialoro, A., Papile, J., Weniger, J., Bethelmie, F., and Tramontano, W.A. 2000. Histone deacetylase inhibitors and cell proliferation in pea root meristems. Phytochemistry, **55**: 11–18.

Nelson, D.A. 1982. Histone acetylation in baker's yeast. Mainte-

© 2002 NRC Canada

nance of the hyperacetylated configuration in log phase protoplasts. J. Biol. Chem. **257**: 1565–1568.

Nightingale, K.P., Wellinger, R.E., Sogo, J.M., and Becker, P.B. 1998. Histone acetylation facilitates RNA polymerase II transcription of the *Drosophila* hsp26 gene in chromatin. EMBO J. **17**: 2865–2876.

Orphanides, G., and Reinberg, D. 2000. RNA polymerase II elongation through chromatin. Nature (Lond.), **407**: 471–476.

Pazin, M.J., and Kadonaga, J.T. 1997. What's up and down with histone deacetylation and transcription? Cell, **89**: 325–330.

Pedersen, T.J., and Minocha, S.C. 1988. Effects of *n*-sodium butyrate on cell division in Jerusalem artichoke *Helianthus tuberosus* L. tuber explants cultured in vitro. J. Plant Physiol. **132**: 623–630.

Ransom, R.F., and Walton, J.D. 1997. Histone hyperacetylation in maize in response to treatment with HC-toxin or infection by the filamentous fungus *Cochliobolus carbonum*. Plant Physiol. **115**: 1021–1027.

Richon, V.M., Sandhoff, T.W., Rifkind, R.A., and Marks, P.A. 2000. Histone deacetylase inhibitor selectively induces p21(WAF1) expression and gene-associated histone acetylation. Proc. Natl. Acad. Sci. U.S.A. **97**: 10 014 – 10 019.

Sanchez-del-Pino, M.M., Lopez-Rodas, G., Sendra, R., and Tordera, V. 1994. Properties of the yeast nuclear histone deacetylase. Biochem. J. **303**: 723–729.

Schroter, H., Gomez-Lira, M.M., Plank, K.-H., and Bode, J. 1981. The extent of histone acetylation induced by butyrate and the turnover of acetyl groups depend on the nature of the cell line. Eur. J. Biochem. **120**: 21–28.

Selker, E.U. 1998. Trichostatin A causes selective loss of DNA methylation in *Neurospora*. Proc. Natl. Acad. Sci. U.S.A. **95**: 9430–9435.

Siavoshian, S., Segain, J.P., Kornprobst, M., Bonnet, C., Cherbut, C., Galmiche, J.P., and Blottiere, H.M. 2000. Butyrate and Trichostatin A effects on the proliferation/differentiation of human intestinal epithelial cells: induction of cyclin D3 and p21 expression. Gut, **46**: 507–514.

Strahl, B.D., and Allis, C.D. 2000. The language of covalent histone modifications. Nature (Lond.), **403**: 41–45.

Vyskot, B., Siroky, J., Hladilova, R., Belaev, N.D., and Turner, B.M. 1999. Euchromatic domains in plant chromosomes as revealed by H4 histone acetylation and early DNA replication. Genome, **42**: 343–350.

Wade, P.A., Jones, P.L., Vermaak, D., Veenstra, G.J., Imhof, A., Sera, T., Tse, C., Ge, H., Shi, Y.B., Hansen, J.C., and Wolffe, A. 1998. Histone deacetylase directs the dominant silencing of transcription in chromatin: association with MeCP2 and the Mi-2 chromodomain SWI/SNF ATPase. Cold Spring Harbor Symp. Quant. Biol. **63**: 435–445.

Waterborg, J.H. 1990. Sequence analysis of acetylation and methylation of two histone H3 variants of alfalfa. J. Biol. Chem. **265**: 17 157 – 17 161.

Waterborg, J.H. 1991. Multiplicity of histone H3 variants in wheat, barley, rice and maize. Plant Physiol. **96**: 453–458.

Waterborg, J.H. 1992*a*. Existence of two histone H3 variants in dicotyledonous plants and correlation between their acetylation and plant genome size. Plant Mol. Biol. **18**: 181–187.

Waterborg, J.H. 1992*b*. Identification of five sites of acetylation in alfalfa histone H4. Biochemistry, **31**: 6211–6219.

Waterborg, J.H. 1993*a*. Histone synthesis and turnover in alfalfa. Fast loss of highly acetylated replacement histone H3.2. J. Biol. Chem. **268**: 4912–4917.

Waterborg, J.H. 1993*b*. Dynamic methylation of alfalfa histone H3. J. Biol. Chem. **268**: 4918–4921.

Waterborg, J.H. 1998. Dynamics of histone acetylation in *Chlamydomonas reinhardtii*. J. Biol. Chem. **273**: 27 602 – 27 609.

Waterborg, J.H. 2000. Steady-state levels of histone acetylation in *Saccharomyces cerevisiae*. J. Biol. Chem. **275**: 13 007 – 13 011.

Waterborg, J.H. 2001. Dynamics of histone acetylation in *Saccharomyces cerevisiae*. Biochemistry, **40**: 2599–2605.

Waterborg, J.H., Harrington, R.E., and Winicov, I. 1987. Histone variants and acetylated species from the alfalfa plant *Medicago sativa*. Arch. Biochem. Biophys. **256**: 167–178.

Waterborg, J.H., Harrington, R.E., and Winicov, I. 1989. Differential histone acetylation in alfalfa (*Medicago sativa*) due to growth in NaCl: Responses in salt stressed and salt tolerant callus cultures. Plant Physiol. **90**: 237–245.

Waterborg, J.H., Harrington, R.E., and Winicov, I. 1990. Dynamic histone acetylation in alfalfa cells. Butyrate interference with acetate labeling. Biochim. Biophys. Acta, **1049**: 324–330.

Waterborg, J.H., Robertson, A.J., Tatar, D.L., Borza, C.M., and Davie, J.R. 1995. Histones of *Chlamydomonas reinhardtii*. Synthesis, acetylation and methylation. Plant Physiol. **109**: 393–407.

Wittschieben, B.O., Otero, G., de Bizemont, T., Fellows, J., Erdjument-Bromage, H., Ohba, R., Li, Y., Allis, C.D., Tempst, P., and Svejstrup, J.Q. 1999. A novel histone acetyltransferase is an integral subunit of elongating RNA polymerase II holoenzyme. Mol. Cell. **4**: 123–128.

Zhang, D.E., and Nelson, D.A. 1988*a*. Histone acetylation in chicken erythrocytes. Rates of acetylation and evidence that histones in both active and potentially active chromatin are rapidly modified. Biochem. J. **250**: 233–240.

Zhang, D.E., and Nelson, D.A. 1988*b*. Histone acetylation in chicken erythrocytes rates of deacetylation in immature and mature red blood cells. Biochem. J. **250**: 241–246.

© 2002 NRC Canada